Acta Cryst. (1982). A**38**, 155–161

The Electronic State of O^{2-} in MgO Studied by the Compton Profile Method

BY O. AIKALA

Department of Physical Sciences, University of Turku, SF-20500 Turku 50, Finland

AND T. PAAKKARI AND S. MANNINEN

Department of Physics, University of Helsinki, SF-00170 Helsinki 17, Finland

(*Received* 2 *June* 1981; *accepted* 11 *September* 1981)

Abstract

The electronic state of the O^{2-} ion in MgO is studied in detail by measuring the isotropic Compton profile and profiles in crystal directions [100], [110], and [111]. The theoretical profiles are calculated using linear combinations of local orbitals orthogonalized to each other symmetrically. The orthogonalization is performed with the 'exact' cluster method. Nine different local wave functions of the O^{2-} ion have been used as the basis of the calculations. The experimental and theoretical profiles as well as their Fourier transforms are compared with each other. The orthogonalized Watson +1 potential-well wave function and the orthogonalized LCAO band function of Pantelides, Mickish & Kunz [*Phys. Rev. B* (1974), **10**, 5203–5212] were found to describe best the ionic state of O^{2-} even though neither of the functions gives complete agreement with the experiment.

1. Introduction

By their chemical nature, the alkaline-earth oxides should lie between the covalent compounds of Groups III–V and the alkali halides with ionic character. Of these alkaline-earth oxides, the bonding mechanism in MgO has been the object of most intensive experimental and theoretical studies. This crystal has the rocksalt structure and general chemical and dielectric considerations demonstrate a strong ionic character for the bonding. The generally assumed configuration $Mg^{2+}O^{2-}$ for the basic constituents is not completely justified because the isolated O^{2-} ion is not a stable one. The existence of O^{2-} in MgO thus implies that this type of constituent must be stabilized by the crystalline field. The simplest way to simulate this field is to replace it by a so called 'Watson sphere', which is a charged hollow sphere with a proper radius. Several such calculations have been performed [*e.g.* wave functions (WF) 4, 5, 6 and 7 in Table 1 and wave functions by Paschalis & Weiss (1969); for criticism concerning these wave functions, see Abarenkov & Antonova (1979)]. More refined wave functions for all states or for the 2*p* state only of O^{2-} have been obtained both by cohesive-energy (*e.g.* WF 1, 2 and 3, as well as a very early and an approximate one, WF 8 in Table 1) and by band-structure calculations (WF 9 in Table 1). The main differences between the various wave functions given in Table 1 are in the 2*p* functions of the O^{2-} ion. Roughly speaking, the wave functions are arranged in Table 1 in an order in which the higher order number means the more extended 2*p* state (*cf.* Fig. 1).

The experimental and theoretical scattering factors of MgO have been compared with each other by Dawson (1969) and by Sanger (1969). The Compton

Table 1. *Wave functions used for the present LCAO calculations for the* MgO *crystal*

The wave functions for the free Mg^{2+} ion of Clementi (1965) and those for the O^{2-} ion of Watson (1958) in the case of +1 potential well have been used unless otherwise stated. The values of $J_{free}(0)$ are calculated from the non-orthogonalized wave functions. References for the wave functions are: WF 1, Yamashita & Asano (1970); WF 2, Abarenkov & Antonova (1979), case II; WF 3, Calais, Mäkilä, Mansikka, Pettersson & Vallin (1971); WF 4, WF 5, Schwarz & Schulz (1978) and Schwarz (1980); WF 6, WF 7, Watson (1958); WF 8, Yamashita & Kojima (1952); WF 9, Pantelides, Mickish & Kunz (1974).

Reference number for the wave functions	$J_{free}(0)$	$J_{isotr}(0)$	Explanation
WF 1	5·931	5·630	O^{2-} (2*p* states).
WF 2	5·963	5·655	O^{2-} (all states).
WF 3	6·193	5·685	O^{2-} (2*p* states).
WF 4	6·110	5·687	O^{2-} (all states): Watson-sphere radius 1·2 Å. The numerical WF's were fitted to STO's by the authors.
WF 5	6·267	5·719	As WF 4, except Watson-sphere radius 1·4 Å.
WF 6	6·202	5·726	O^{2-} (all states): +2 potential well.
WF 7	6·349	5·750	O^{2-} (all states): see WF 6, + 1 potential well.
WF 8	6·330	5·803	O^{2-} (2*p* states).
WF 9	6·459	5·813	MH^{2+} (all states), O^{2-} (all states).

0567-7394/82/010155-07$01.00

profiles have been compared by Togawa, Inkinen & Manninen (1971), Weiss (1970) and Fukamachi & Hosoya (1971). However, the earlier experimental data on Compton profiles were not corrected for multiple scattering effects. All these comparisons are not adequate for the theoretical consideration because the strong non-orthogonality of the wave functions is not considered. This was done in the calculations by Mansikka & Aikala (1973) [*cf.* also Aikala (1974) and Berggren, Manninen, Paakkari, Aikala & Mansikka (1977)] in an approximate way including the first two terms in the binomial series of the orthogonalization corrections. However, this approximation has been found unsatisfactory because of the large overlap between the adjacent O^{2-} ions (Aikala, 1980).

The atomic charge densities in MgO have been studied by Vidal-Valat, Vidal & Kurki-Suonio (1978) on the basis of Sanger's (1969) structure factor data. Recently, Redinger & Schwarz (1981) have compared the SCF APW charge densities in MgO to the free-ion densities calculated within the Watson-sphere model and found an excellent agreement. However, in neither of these works was the non-orthogonality of the free-ion wave functions considered.

On a purely theoretical basis the wave functions 1, 2, 3 and 9 should be the best ones. This is a contradictory claim because the $2p$ states of O^{2-} differ very much in these wave functions (*cf.* Fig. 1).

In this paper reliable experimental Compton profile data are given in various crystal directions. The theoretical profiles are calculated within the LCAO approximation by applying the 'exact' cluster orthogonalization procedure (Aikala, 1980) to the various basis functions presented in Table 1. The orthogonality is a necessary but not sufficient condition for the true crystal wave functions; the quality of the various wave functions in Table 1 depends on the validity of the approximations made in the calculations (see references in Table 1). The experimental and theoretical results are finally compared with each other to study the ionic state of the O^{2-} ion, with special attention to the $2p$ state.

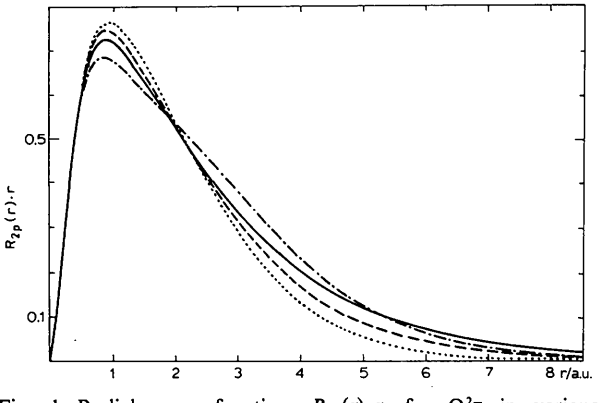

Fig. 1. Radial wave function, $R_{2p}(r).r$, for O^{2-} in various theoretical approximations: Watson (WF 7, solid line), Abarenkov & Antonova (WF 2, dotted line), Schwarz & Schulz (WF 4, broken line) and Pantelides *et al.* (WF 9, broken–dotted line).

2. Experimental

Compton profiles were measured using 59·537 keV γ-rays from a ^{241}Am annular source [nominal activity 5 Ci (19×10^{10} Bq)]. The scattering angle was 174·5° and the resolution of the spectrometer 0·6 a.u. (FWHM). An isotropic profile was also measured using a scattering angle of 166°. Details of experimentation and data processing have been published previously (Manninen & Paakkari, 1978; Paatero, Manninen & Paakkari, 1974; Halonen, Williams & Paakkari, 1975).

Thin (0·75 mm) slices were cut from a single crystal of MgO along the crystal planes (100), (110) and (111). For powder samples, high-purity MgO powder was heated for several hours at 753 K to decompose $Mg(OH)_2$. The absence of $Mg(OH)_2$ in powder samples and the perfectness of single-crystal samples was proved by X-ray diffraction.

The total number of counts collected for each sample was about 15×10^6, which corresponded to a peak count of 3×10^5 with a channel spacing of 0·1 a.u. of momentum. Data were corrected for the effects of background, absorption in the sample, the energy dependence of the differential cross section, and the experimental resolution. The contribution of double Compton scattering was calculated using a Monte Carlo program. The total amount was about 2% and 7% and its effect at $J(0)$ 0·4% and 0·9% for powder and single-crystal samples, respectively. In difference curves the effects of all of these corrections were very small.

It was also found that the correction applied for double scattering was negligible when $z > 3$ a.u. in the Fourier transforms of the profiles, $B(z)$. The correction had no effect on the anisotropy of $B(z)$, *i.e.* the difference curves. This is understandable because the profile of the double scattering is very flat and thus contributes to $B(z)$ only at low values of z.

The direction of the scattering vector deviates systematically on average by three degrees from the exact crystal direction in the present experimental arrangement. In fact, the scattering vector always lies on a surface of a cone, the axis of which is parallel to the reported crystal direction. Aikala (1981) has shown that this deviation together with the beam divergences (5° FWHM) has a negligible effect on the experimental anisotropy curves in the present case.

3. Theoretical

Within the LCAO model the first-order density matrix $\rho(\mathbf{r},\mathbf{r}')$ for the crystal composed of 'closed-shell' constituents is given by (Löwdin, 1955):

$$\rho(\mathbf{r},\mathbf{r}') = \sum_{\mu}\sum_{\nu} \Psi_{\mu}(\mathbf{r})\,(\mathbb{\Delta}^{-1})_{\mu\nu}\,\Psi_{\nu}^{*}(\mathbf{r}') \qquad (1)$$

when local orbitals $\Psi_{\mu}(\mathbf{r})$, which are supposed to be known, are used as the basis. In (1) $\mathbb{\Delta}^{-1}$ is the inverse of the metric matrix $\mathbb{\Delta}$ with elements

$$\Delta_{\mu\nu} = \int \Psi_{\mu}^{*}(\mathbf{r})\,\Psi_{\nu}(\mathbf{r})\,\mathrm{d}^3\,\mathbf{r}. \qquad (2)$$

So far, mainly the binomial series expansion for $\mathbb{\Delta}^{-1}$ in $\mathbb{S} = \mathbb{\Delta} - \mathbb{1}$ ($\mathbb{1}$ is the unit matrix) has been used. $\mathbb{S}$ is called the overlap matrix. Recently, one of the authors has used a cluster method to calculate $\mathbb{\Delta}^{-1}$ more accurately (Aikala, 1980). The method is based on the equation

$$\mathbb{T}\,\mathbb{\Delta} = \mathbb{1} \quad (\mathbb{T} = \mathbb{\Delta}^{-1}) \qquad (3)$$

and the site symmetries of the atoms/ions in the crystal are exploited completely to make the problem tractable.

The momentum density $\rho(\mathbf{p})$ can then be obtained as the double Fourier transform of $\rho(\mathbf{r},\mathbf{r}')$ given by equation (1). The Compton profile $J_{\mathbf{k}}(p_z)$ in the direction $\mathbf{k}$ is by definition the one-dimensional projection of the momentum density on the line defined by the scattering vector $\mathbf{k}$ (see *e.g.* Williams, 1977). The details for computing the Compton profiles from the first-order density matrix (1) are given elsewhere (Aikala, 1975*a*, 1975*b*, 1976, 1977).

The Fourier transforms $B_{\mathbf{k}}(z)$ of the theoretical (and experimental) Compton profiles $J_{\mathbf{k}}(p_z)$ can then be calculated with standard FFT (Fast Fourier Transform) programs.

4. Results and discussion

The experimental isotropic Compton profile of MgO is given in Table 2 together with a theoretical profile calculated using WF 7. The area under the curve is normalized to 9·6049 e for $p_z = [0,7]$ using steps of 0·1 a.u. The differences between the experimental profile (θ = 166° in Table 2) and some theoretical profiles after convolution with the RIF (Residual Instrument Function) of the experiment are given in Fig. 2. These are chosen to represent all the typical features of the various curves and the most recently published wave functions have been taken as the representatives.

WF 1 and WF 2 give mutually similar profiles as do pairs WF 8 and WF 9, WF 3 and WF 4, and WF 5 and WF 6. The difference in the two last mentioned pairs is, however, rather small. The best agreement is obtained with the profiles calculated using WF 7 and WF 9 as the basis. It is an interesting feature that these functions give opposite signs to the difference in the regions where largest discrepancies between theory and experiment occur.

The present theoretical results can be compared with the series expansion results by Mansikka & Aikala (1973) (see also Berggren *et al.*, 1977). These profiles are flat in comparison with the present 'exact' ones. For instance, $J^{1}_{\mathrm{ser,isotr}}(0) = 5{\cdot}575$ and $J^{1}_{\mathrm{isotr}}(0) = 5{\cdot}630$ for WF 1 and $J^{7}_{\mathrm{ser,isotr}}(0) = 5{\cdot}597$ and $J^{7}_{\mathrm{isotr}}(0) = 5{\cdot}750$ for WF 7. Thus the series expansion orthogonalization is a poor approximation for MgO, at least in terms of the Compton profile. This is not the case when typical ionic solids like LiF are considered (Aikala, 1979*a*). This fact is partially responsible for the previously found

Table 2. *The experimental, isotropic Compton profile of* MgO

The result obtained at the scattering angle of 175° is given for comparison. The theoretical profile, $J^{7}(p_z)$, is calculated using WF 7. The residual instrument function (RIF) and its Fourier transform (RAF) correspond to the value 30 of the deconvolution parameter λ (see Paatero, Manninen & Paakkari, 1974). The values of p_z and z are in atomic units and the statistical error (3σ) is given at some points.

	$J(p_z)_{\mathrm{isotr}}$			RIF		RAF
p_z	166°	175°	$J^{7}(p_z)$	(λ=30)	z	(λ=30)
0·0	5·774	5·770	5·750	1·600	0·0	1·000
	±0·025					
0·1	5·751	5·739	5·728	1·522	0·25	0·999
0·2	5·676	5·664	5·660	1·304	0·5	0·997
0·3	5·551	5·546	5·545	0·995	0·75	0·994
0·4	5·376	5·382	5·379	0·641	1·0	0·990
0·5	5·156	5·174	5·160	0·314	1·25	0·987
0·6	4·894	4·922	4·898	0·056	1·5	0·985
0·7	4·598	4·632	4·604	−0·112	1·75	0·984
0·8	4·277	4·309	4·284	−0·190	2·0	0·983
0·9	3·943	3·968	3·948	−0·195	2·25	0·982
1·0	3·604	3·619	3·606	−0·154	2·5	0·978
	±0·020					
1·1	3·273	3·278	3·271	−0·091	2·75	0·970
1·2	2·956	2·954	2·955	−0·031	3·0	0·958
1·3	2·664	2·658	2·668	0·014	3·25	0·933
1·4	2·400	2·395	2·415	0·039	3·5	0·900
1·5	2·167	2·169	2·196	0·046	3·75	0·858
1·6	1·964	1·976	2·008	0·040	4·0	0·795
1·7	1·791	1·811	1·847	0·026	4·25	0·732
1·8	1·644	1·669	1·705	0·012	4·5	0·660
1·9	1·519	1·546	1·578	0·000	4·75	0·581
2·0	1·412	1·433	1·462	−0·008	5·0	0·497
2·2	1·233	1·238	1·260	−0·010	5·25	0·412
2·4	1·081	1·073	1·092	−0·004	5·5	0·337
2·6	0·947	0·938	0·952	0·001	5·75	0·264
2·8	0·828	0·825	0·836	0·002	6·0	0·200
3·0	0·733	0·726	0·737	0·001	6·25	0·150
	±0·010					
3·5	0·554	0·540	0·547	−0·001	6·5	0·107
4·0	0·425	0·418	0·417		6·75	0·082
4·5	0·335	0·330	0·329		7·0	0·051
5·0	0·273	0·271	0·263		7·25	0·036
6·0	0·184	0·181	0·176		7·5	0·025
7·0	0·128	0·127	0·122			

Table 3. *Theoretical and experimental Compton profiles of* MgO *in the directions* [100], [110] *and* [111]

The theoretical profiles are calculated using WF 7 and integrated with the method explained by Aikala (1977, p. 50). 21 orders of neighbours are included and the numbers of the Gauss–Legendre integration points are 96 for p_z = [0,2], 64 for p_z = [2·2,4] and 48 for $p_z > 4$ a.u.

p_z	$J^T_{(100)}$	$J^T_{(110)}$	$J^T_{(111)}$	$J^{exp}_{(100)}$	$J^{exp}_{(110)}$	$J^{exp}_{(111)}$
0·0	5·748	5·680	5·706	5·700	5·681	5·667
0·1	5·730	5·692	5·720	5·666	5·650	5·643
0·2	5·668	5·672	5·688	5·589	5·575	5·577
0·3	5·549	5·568	5·558	5·468	5·459	5·470
0·4	5·368	5·397	5·387	5·302	5·300	5·316
0·5	5·135	5·175	5·189	5·093	5·100	5·114
0·6	4·861	4·902	4·932	4·843	4·861	4·871
0·7	4·558	4·594	4·621	4·558	4·585	4·588
0·8	4·237	4·285	4·285	4·249	4·282	4·275
0·9	3·913	3·982	3·935	3·926	3·957	3·944
1·0	3·593	3·657	3·576	3·600	3·621	3·603
1·1	3·287	3·303	3·232	3·279	3·285	3·265
1·2	3·003	2·948	2·925	2·974	2·963	2·944
1·3	2·746	2·633	2·655	2·692	2·664	2·649
1·4	2·509	2·373	2·410	2·435	2·396	2·385
1·5	2·281	2·158	2·190	2·205	2·165	2·132
1·6	2·062	1·977	2·004	2·000	1·968	1·967
1·7	1·862	1·826	1·851	1·821	1·802	1·807
1·8	1·689	1·698	1·715	1·665	1·665	1·672
1·9	1·543	1·581	1·585	1·530	1·548	1·553
2·0	1·418	1·473	1·465	1·415	1·447	1·450
2·2	1·220	1·292	1·266	1·224	1·269	1·262
2·4	1·069	1·101	1·097	1·078	1·106	1·097
2·6	0·947	0·951	0·955	0·959	0·955	0·956
2·8	0·845	0·823	0·837	0·860	0·831	0·840
3·0	0·756	0·731	0·734	0·768	0·737	0·740
3·5	0·547	0·550	0·546	0·548	0·557	0·552
4·0	0·410	0·414	0·417	0·431	0·435	0·436
4·5	0·329	0·330	0·329	0·343	0·341	0·342
5·0	0·266	0·261	0·263	0·275	0·276	0·281
6·0	0·175	0·176	0·176	0·191	0·188	0·191
7·0	0·122	0·122	0·122	0·133	0·133	0·133

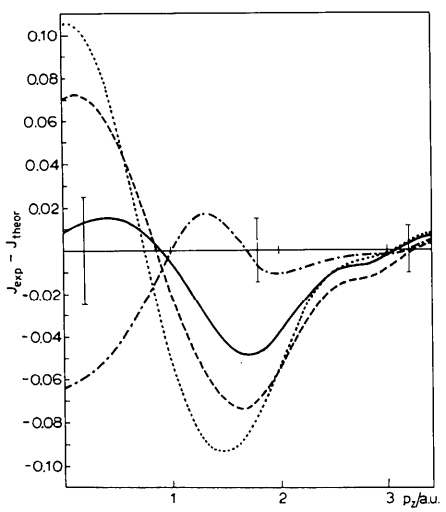

Fig. 2. Differences between the experimental and theoretical isotropic Compton profiles of MgO. For theoretical profiles the wave functions mentioned in the caption of Fig. 1 have been used.

disagreement between theory and experiment (see Berggren *et al.*, 1977).

The directional Compton profiles were calculated using the same method and the same wave functions as the isotropic profiles. As an example, the directional profiles in the crystal directions [100], [110], and [111], calculated using WF 7, are given in Table 3 together with the present experimental profiles.

The experimental and convoluted (with RIF given in Table 2) theoretical anisotropies $J_{(110)} - J_{(100)}$ and $J_{(111)} - J_{(110)}$ are compared in Figs. 3 and 4. The experimental anisotropies are given as an average of the values of the profile at positive and negative p_z. The agreement is found to be rather good except at low values of p_z where some deviations occur. The various theoretical curves differ little from each other, most when $p_z < 1$. If these anisotropies are compared with those of alkali halides with the same NaCl structure (Berggren, Martino, Eisenberger & Reed, 1976; Aikala & Salonen, 1978; Aikala, 1979*b*) they are found to resemble each other. Thus the main features of the anisotropy can be deduced to depend on the structure likewise in the case of alkali halides (Aikala, 1979*b*)

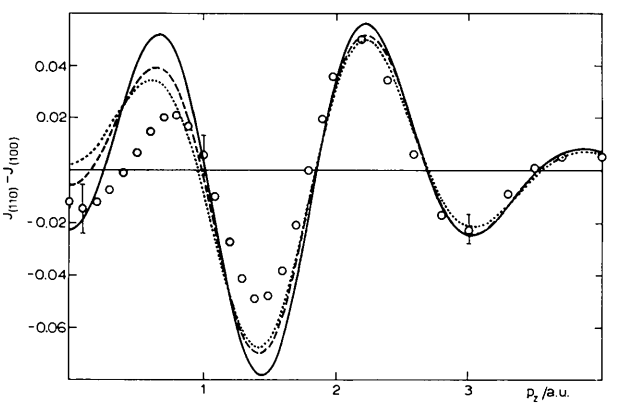

Fig. 3. Difference between the directional profiles $J_{(110)} - J_{(100)}$. The experimental result is given by circles and the experimental errors are indicated at some points. The theoretical results are given using wave functions by Watson (WF 7, solid line), Abarenkov & Antonova (WF 2, dotted line) and Schwarz & Schulz (WF 4, broken line).

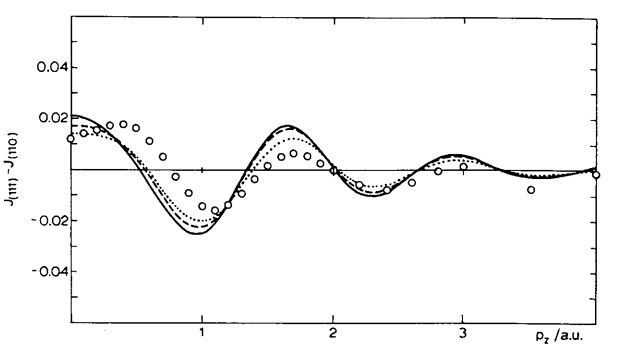

Fig. 4. Difference between the directional profiles $J_{(111)} - J_{(110)}$. For further explanation, see caption for Fig. 3.

and other NaCl structures (Seth, Paakkari, Manninen & Christensen, 1977).

The Fourier transforms of the isotropic and directional profiles were also calculated and compared with the experimental data (Figs. 5–9). In Fig. 5 the isotropic $B(z)$ functions are shown. The experimental and theoretical curves agree quite well, although the minimum at $z = 4{\cdot}3$ a.u. is correctly produced only when WF 9 is used. In the case of $B_{(100)}$ (Fig. 6) the theoretical functions differ noticeably from each other and from the experimental one when $3{\cdot}5 \leq z \leq 5$ a.u. In the experimental curve a shallow (double) minimum can be seen. The second minimum is reproduced by all theoretical wave functions. At the position of the first minimum the theoretical curves have only shoulders of various heights except in the curve corresponding to WF 9 where there is only a change of the slope. To clarify this feature various approximations for the theoretical $B_{(100)}$ are drawn in Fig. 8 using WF 1. It should be mentioned that the one-center orthogonalization contribution is included in all of the curves excluding the free-ion curve. Inclusion of the first two orders of neighbours produces almost completely the 'exact' curve. Further, the second neighbours are seen to be responsible for the shoulder or, if the series expansion approximation is considered, the minimum of the $B_{(100)}$ curve. The series approximation produces larger elements for the inverse metric matrix than the 'exact' inversion. Thus an enlargement of the 'exact' elements might replace the shoulder by a minimum. On the other hand, such changes in the wave functions which produce larger inverse metric matrix elements will also cause other changes to the course of the $B_{(100)}$ curve. The minimum is not then produced, but instead the shoulder occurs higher, which can be seen by comparing corresponding curves in Figs. 1 and 6.

In Fig. 9 the differences $B_{(110)} - B_{(100)}$ and $B_{(111)} - B_{(110)}$ are shown. The agreement between theory and experiment is reasonable except close to the origin. On the other hand, the possibility of some systematic error in the experimental curves is larger in this region. The most contracted wavefunction WF 2 (which produces

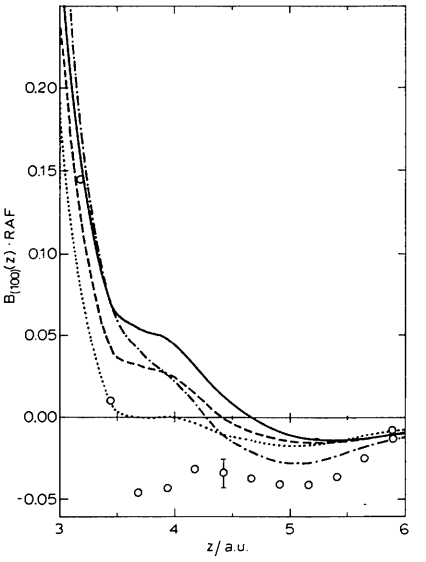

Fig. 6. Fourier transform of the Compton profile in the crystal direction [100]. Circles give the experimental result; for other explanations, see caption for Fig. 1.

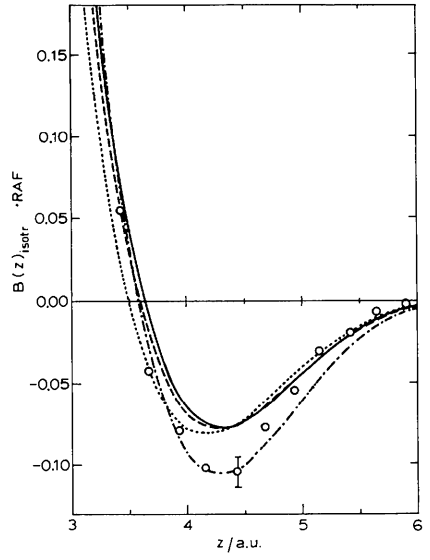

Fig. 5. Fourier transform of the isotropic Compton profile of MgO, $B(z)_{\text{isotr}}$. Circles give the experimental result; for other explanations, see caption for Fig. 1.

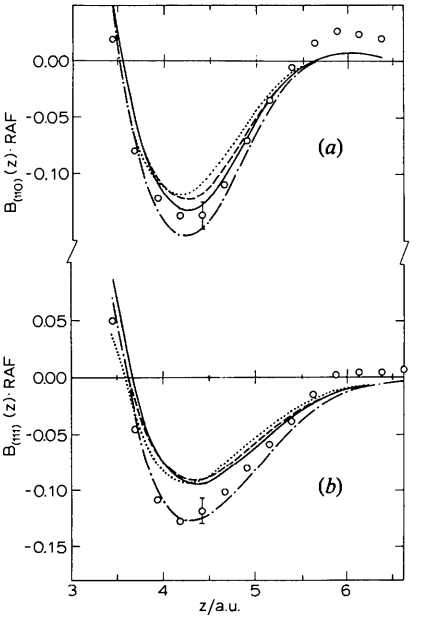

Fig. 7. Fourier transforms of the Compton profile in crystal directions (*a*) [110], (*b*) [111]. Circles give the experimental result; for other explanations, see caption for Fig. 1.

the smallest inverse metric matrix elements) is seen to give correctly the minimum at $z \simeq 4$ a.u. in Fig. 9(*a*). Thus the difference found between the experimental and theoretical $B_{(100)}$ curves near $z \simeq 4$ a.u. can be of isotropic nature, at least in the case of WF 2. Indeed, a similar difference is also found in the isotropic $B(z)$ curves.

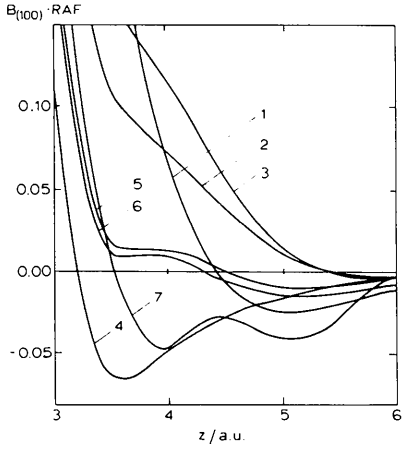

Fig. 8. Effects of the neighbours upon the Fourier-transformed Compton profile of MgO in the direction [100]. Wavefunctions given by Yamashita & Asano (WF 1) have been used for this calculation for the O^{2-} ion. Explanation of numbered curves: (1) $B_{(100)}$ for free ions; (2) series expansion up to first neighbours; (3) exact result up to first neighbours; (4) series expansion up to second neighbours; (5) exact result up to second neighbours; (6) the exact result for $B_{(100)}$ when all 21 orders of the neighbours are taken into account; (7) experimental result.

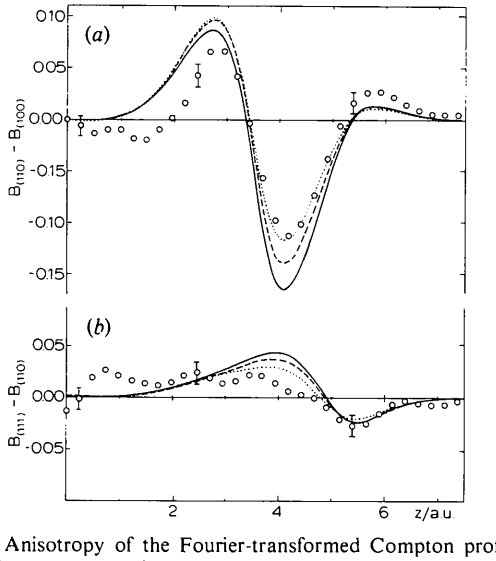

Fig. 9. Anisotropy of the Fourier-transformed Compton profiles. (*a*) $B_{(110)} - B_{(100)}$, (*b*) $B_{(111)} - B_{(110)}$. For further explanations, see caption for Fig. 3.

Redinger & Podloucky (1981) have calculated the Compton profiles of MgO with the self-consistent APW method. Their results are close to those obtained using WF 9 which are based on the LCAO band calculation. Thus both of the methods seem to give results compatible with the Compton profiles. On the other hand, all cohesive-energy calculations seem to give mutually similar results which deviate from the results of the band calculation. The band calculation (WF 9) seems to give Compton profiles which are in better agreement with the experiment than any of the cohesive-energy calculations (WF 1–WF 3). The reason why the cohesive-energy calculations fail in this respect is not known; in some cases the reason might be the lack of flexibility of the basis.

In conclusion one can say that none of the wave functions 1–9 when orthogonalized reproduces all features of the experiment completely, but the best ones are the Watson +1 well and the LCAO band function of Pantelides *et al.* (WF 9), whereas the functions obtained by cohesive-energy calculations give the worst agreement between theory and experiment.

The authors wish to thank Drs R. Podloucky and J. Redinger for sending their data prior to publication and Professor K. Schwarz for the numerical wavefunctions for O^{2-}. Miss R. Ström and Miss M.-L. Putkonen have given valuable help in the computations. TP and SM are indebted to the National Research Council for Science, Finland, for financial support.

References

ABARENKOV, I. V. & ANTONOVA, I. M. (1979). *Phys. Status Solidi B*, **93**, 315–323.
AIKALA, O. (1974). *J. Phys. C*, **7**, L40–L43.
AIKALA, O. (1975*a*). *Philos. Mag.* **31**, 935–942.
AIKALA, O. (1975*b*). *Philos. Mag.* **32**, 333–341.
AIKALA, O. (1976). *Philos. Mag.* **33**, 603–611.
AIKALA, O. (1977). Report D1. Department of Physical Sciences, Univ. of Turku, Turku, Finland.
AIKALA, O. (1979*a*). *J. Phys. C*, **12**, L581–L585.
AIKALA, O. (1979*b*). *Solid State Commun.* **32**, 699–701.
AIKALA, O. (1980). *J. Phys. C*, **13**, 5931–5939.
AIKALA, O. (1981). To be published.
AIKALA, O. & SALONEN, K. (1978). Report No. R6. Department of Physical Sciences, Univ. of Turku, Turku, Finland.
BERGGREN, K.-F., MANNINEN, S., PAAKKARI, T., AIKALA, O. & MANSIKKA, K. (1977). *Compton Scattering*, edited by B. WILLIAMS. London: McGraw-Hill.
BERGGREN, K.-F., MARTINO, F., EISENBERGER, P. & REED, W. A. (1976). *Phys. Rev. B*, **13**, 2292–2304.
CALAIS, J. L., MÄKILÄ, K., MANSIKKA, K., PETTERSSON, G. & VALLIN, J. (1971). *Phys. Scr.* **3**, 39–42.
CLEMENTI, E. (1965). *Tables of Atomic Functions*. Suppl. to *IBM J. Res. Dev.* **9**, 2–19.
DAWSON, B. (1969). *Acta Cryst.* A**25**, 12–29.

FUKAMACHI, T. & HOSOYA, S. (1971). *J. Phys. Soc. Jpn*, **31**, 980–989.
HALONEN, V., WILLIAMS, B. & PAAKKARI, T. (1975). *Phys. Fenn.* **10**, 107–122.
LÖWDIN, P. O. (1955). *Phys. Rev.* **97**, 1490–1508.
MANNINEN, S. & PAAKKARI, T. (1978). *Nucl. Instrum. Methods*, **155**, 115–119.
MANSIKKA, K. & AIKALA, O. (1973). *Ann. Univ. Turku. Ser. A* 1, pp. 43–55.
PAATERO, P., MANNINEN, S. & PAAKKARI, T. (1974). *Philos. Mag.* **30**, 1281–1294.
PANTELIDES, S. T., MICKISH, D. J. & KUNZ, A. B. (1974). *Phys. Rev. B*, **10**, 5203–5212.
PASCHALIS, E. & WEISS, A. (1969). *Theor. Chim. Acta*, **13**, 381–408.
REDINGER, J. & PODLOUCKY, R. (1981). Private communication.
REDINGER, J. & SCHWARZ, K. (1981). *Z. Phys. Chem. Abt. B*, **40**, 269–276.
SANGER, P. L. (1969). *Acta Cryst.* A**25**, 694–702.
SCHWARZ, K. (1980). Private communication.
SCHWARZ, K. & SCHULZ, H. (1978). *Acta Cryst.* A**34**, 994–999.
SETH, A., PAAKKARI, T., MANNINEN, S. & CHRISTENSEN, A. N. (1977). *J. Phys. C*, **10**, 3127–3139.
TOGAWA, S., INKINEN, O. & MANNINEN, S. (1971). *J. Phys. Soc. Jpn*, **30**, 1132–1135.
VIDAL-VALAT, G., VIDAL, J. P. & KURKI-SUONIO, K. (1978). *Acta Cryst.* A**34**, 594–602.
WATSON, R. E. (1958). *Phys. Rev.* **111**, 1108–1110.
WEISS, R. J. (1970). *Philos. Mag.* **21**, 1169–1173.
WILLIAMS, B. G. (1977). Editor. *Compton Scattering*. London: McGraw-Hill.
YAMASHITA, J. & ASANO, S. (1970). *J. Phys. Soc. Jpn*, **28**, 1143–1150.
YAMASHITA, J. & KOJIMA, M. (1952). *J. Phys. Soc. Jpn*, **7**, 261–263.

Short Communications

Contributions intended for publication under this heading should be expressly so marked; they should not exceed about 1000 *words; they should be forwarded in the usual way to the appropriate Co-editor; they will be published as speedily as possible.*

Acta Cryst. (1982). A**38**, 161–163

The rapid computation of mean path length for spheres and cylinders.

By J. E. TIBBALLS, *Department of Physics, University of Edinburgh, The King's Buildings, Mayfield Road, Edinburgh EH9 3JZ, Scotland*

(*Received* 3 *April* 1981; *accepted* 16 *June* 1981)

Abstract

Extension of the interpolation formulae of Dwiggins [*Acta Cryst.* (1975), A**31**, 146–148] for the rapid calculation of absorption corrections is shown to allow the equally rapid calculation of the mean path length, $\bar{T}$, required for extinction corrections. The coefficients required to set up the calculations are tabulated. They approximate $\bar{T}$ to within 0·5% R at low 2θ and 2% R at $\theta = 90°$ for $\mu R \leq 2{\cdot}5$ and also provide the derivatives required to estimate μR by the least-squares analysis of powder diffraction profiles for $\mu R > 1$.

Accurate analyses of X-ray and neutron diffraction data require correction of individual intensities for extinction in the sample. The correction requires knowledge of the mean path length of the beam

$$\bar{T} = \frac{1}{VA} \int_V t e^{-\mu t} \, dV, \qquad (1)$$

where t is the path length in a crystal with absorption coefficient μ of a ray scattered in volume element dV. For a general shape, the mean path length $\bar{T}$ is evaluated in conjunction with the computation of the transmission factor A by numerical integration.

For two cases, of the spherical sample in any orientation and the cylindrical sample when data is collected in the plane normal to its axis, tabulation of the calculations is feasible. Bond (1959), Rouse, Cooper, York & Chakera (1970) and subsequently Dwiggins (1975*a*,*b*) provided values of $A^* \equiv 1/A$ for values of the scattering angle θ, and the product, μR, of the absorption coefficient and the sample radius. Pryor & Sanger (1970) obtained values of $\bar{T}$ for spheres by Gaussian integration for $\mu R \leq 10$ while Flack & Vincent (1978) employed numerical differentiation of Dwiggin's (1975*b*) tabulation for $\mu R \leq 2{\cdot}5$. Rouse *et al.* (1970) and Dwiggins (1975*a*) provide analytical approximations for μR less than 1 and 2·5, respectively.

In this note we show that Dwiggins's (1975*a*) approximation formulae may be extended to cover A^* and $\bar{T}$ for both spheres and cylinders, obtaining an accuracy of 0·5% in A^* and achieving the accuracy in $\bar{T}$ necessary for extinction

0567-7394/82/010161-03$01.00